Mutational Analysis of the Subunit Interface of *Vibrio harveyi* Bacterial Luciferase[†,‡]

Jennifer K. Inlow[§] and Thomas O. Baldwin*

Department of Biochemistry and Molecular Biophysics, The University of Arizona, Tucson, Arizona 85721-0088

Received December 4, 2001

ABSTRACT: Bacterial luciferase is a heterodimeric ($\alpha\beta$) enzyme which catalyzes a light-producing reaction in *Vibrio harveyi*. In addition to the $\alpha\beta$ enzyme, the β subunit can self-associate to form a stable but inactive homodimer [Sinclair, J. F., Ziegler, M. M., and Baldwin, T. O. (1994) *Nat. Struct. Biol. 1*, 320−326]. The studies reported here were undertaken to explore the role of the subunit interface in the conformational stability of the enzyme. To this end, we constructed four mutant heterodimers in which residues at the subunit interface were changed in an effort to alter the volume of an apparent solvent accessible channel at the interface or to alter H-bonding groups. Equilibrium unfolding data for the heterodimer have been interpreted in terms of a three-state mechanism [Clark, C. A., Sinclair, J. F., and Baldwin, T. O. (1993) *J. Biol. Chem*. *268*, 10773−10779]. However, we found that unfolding for the wild-type and mutant luciferases is better described by a four-state model. This change in the proposed mechanism of unfolding is based on observation of residual structure in the subunits following dissociation of the heterodimeric intermediate. All of the mutants display modest reductions in activity but, surprisingly, no change in the $\Delta G_2^{H_2O}$ value for subunit dissociation and no measurable change in the equilibrium dissociation constant relative to that of the wild-type heterodimer. However, the $\Delta G_1^{H_2O}$ value for the formation of the dimeric intermediate that precedes subunit dissociation is reduced for three of the mutants, indicating that mutations at the interface can alter the stability of a region of the α subunit that is distant from the interface. We conclude that the interface region communicates with the distal domains of this subunit, probably through the active center region of the enzyme.

Vibrio harveyi luciferase is a heterodimeric ($\alpha\beta$) flavin monooxygenase with a molecular mass of ∼77 kDa (*1*, *2*). The β subunit can self-associate to form a homodimer that has essentially no activity (*3*−*5*). The crystal structures for both the heterodimer (1.5 Å) (*6*) and homodimer (1.95 Å) have been reported (*7*), showing that the α and β subunits, which are homologous (*8*), each adopt the same $(\beta/\alpha)_8$ barrel structure. The structures of the two dimers superimpose extremely well (1.99 Å rms deviation), demonstrating that the β subunit adopts the same fold whether it is associated with the α subunit or another β subunit.

It is of interest that the luciferase subunits do not fold by the same mechanism (*5*, *9*, *10*), even though they have the same three-dimensional structure (*6*, *7*) and are homologous (*8*), with 36% of the sequence being identical (*1*, *2*). The folding of the heterodimer has been described by a three-state mechanism

$$(\alpha\beta)_N \overset{K_1}{\rightleftharpoons} (\alpha\beta)_I \overset{K_2}{\rightleftharpoons} \alpha_U + \beta_U$$

involving an inactive dimeric intermediate in addition to the native state and the unfolded subunits (*9*). The β_2 homodimer has an apparent two-state folding mechanism with a large hysteresis (6 M urea) between its unfolding and refolding transitions, resulting from extremely slow folding and unfolding rates (*5*). The conformational stabilities of the heterodimer and homodimer are approximately the same, but the rates of formation are vastly different; the heterodimer forms with a rate constant of ∼2400 M^{-1} s^{-1} in 50 mM phosphate buffer at pH 7.0 and 18 °C (*10*), while the β subunit self-associates much more slowly under the same conditions, forming the homodimer with a rate constant of ∼180 M^{-1} s^{-1} (*5*). If the α subunit is available, the heterodimer is the kinetically preferred folding product as a result of this great difference in association rates. Nature apparently has used the difference in folding and assembly mechanism between these two structurally similar dimers to preclude the formation of the biologically inactive homodimer. This example underscores the importance of kinetics in achieving the biologically active native state.

The structural basis for the vast difference in association rate constants is unknown, but it appeared to be reasonable to suggest that the subunit interface might play a central role in determining the rate of association. There is a high degree

[†] This work was supported in part by a grant from the National Science Foundation (MCB-0078363).

[‡] This work comprised a portion of the Ph.D. work of J.K.I. submitted to the graduate college of Texas A&M University.

* To whom correspondence should be addressed: Department of Biochemistry and Molecular Biophysics, The University of Arizona, Tucson, AZ 85721-0088. Phone: (520) 621-9185. Fax: (520) 626-9204. E-mail: tbaldwin@u.arizona.edu.

[§] Current address: Arizona Research Laboratories, Division of Neurobiology, The University of Arizona, Gould-Simpson 611, P.O. Box 210077, Tucson, AZ 85721-0077.

10.1021/bi012113g CCC: $22.00 © 2002 American Chemical Society
Published on Web 02/27/2002

of similarity between the subunit interface regions of the heterodimer and homodimer, in both sequence and structural features. Of the 102 identical residues between α and *β*, approximately 25% are at the subunit interface (*6*). The nature and amount of buried surface area are similar for the two dimers, 4250 Å^2 for the heterodimer and 3970 Å^2 for the homodimer. The hydrogen bonding pattern is also similar across the interface of the two dimers. There are 22 intersubunit hydrogen bonds and 45 water-mediated hydrogen bonds at the interface of the heterodimer, and 16 intersubunit and 30 water-mediated hydrogen bonds at the homodimer subunit interface (*7*).

Despite this similarity, there are a few interesting differences between the subunit interfaces of the heterodimer and homodimer. There is a large solvent accessible pocket located at the interface between the two subunits of the luciferase dimer, where many ordered water molecules are observed (*6*, *7*). In the heterodimer (Figure 1A), this pocket extends to the center of the molecule, approximately 20 Å from the external surface of the subunit interface (*6*). The solvent accessible pocket of the homodimer extends only half as far into the molecule as it does in the heterodimer, or approximately one-quarter of the diameter of the interface (∼10 Å), because the inner region of the pocket is isolated from the external solvent by several amino acid side chains (Figure 1B; compare with Figure 1A) (*7*).

To investigate the role of the subunit interface in contributing to the differences in the behavior of the heterodimer and homodimer, we constructed four mutants that alter the subunit interface region of the proteins. We mutated four of the subunit interface residues (α-Ala81, *β*-His81, *β*-His82, and *β*-Glu89). The histidinyl residue at *β*81 is one of the residues responsible for isolating the inner portion of the solvent accessible pocket from the external solvent in the homodimer (*7*). In the heterodimer, α-Ala81 lies across the subunit interface from *β*-His81 (*6*). The glutamyl residue at position *β*89 is located in the inner portion of the pocket, while *β*-His82 is located on the outer edge of the solvent accessible pocket (*6*).

Figure 2 shows the opening of the solvent accessible pocket in both the heterodimer and homodimer with the surface area contributed by residue 81 (histidine in *β* and alanine in α) highlighted. In the heterodimer, the *β*-His81 and α-Ala81 side chains are opposite each other across the interface with the narrow channel of the solvent accessible pocket between them. In contrast, in the homodimer, the two His81 side chains are close together across the interface so that they are partially responsible for isolating the inner portion of the solvent accessible pocket. This can be seen in panels A and B of Figure 1, which show the orientation of the side chains of residue 81 across the interface from each other in the heterodimer and homodimer, respectively. To determine if this occlusion of the solvent accessible pocket makes an important contribution to the differences between the heterodimer and homodimer, we constructed two single-site mutants of the heterodimer at position 81, changing His81 in *β* to alanine and Ala81 in α to histidine (α-A81H and *β*-H81A). The α-A81H mutant heterodimer should have a solvent accessible pocket similar to that of the homodimer since there are two histidine residues opposite each other near the middle of the pocket. The *β*-H81A mutant heterodimer should have a widened solvent accessible pocket relative to that of the wild-type heterodimer because there are two alanine side chains opposite each other across the interface, rather than a histidine and an alanine side chain.

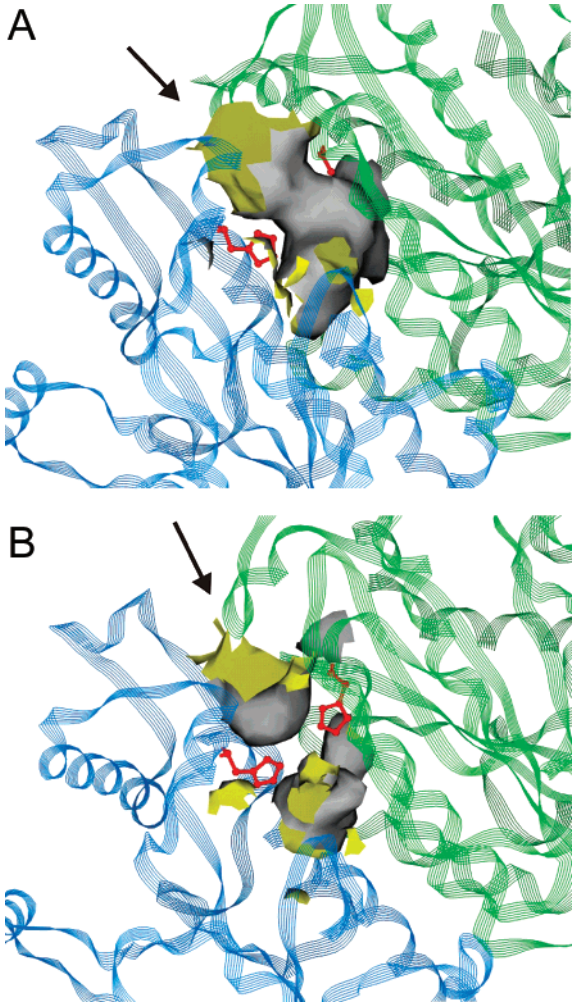

FIGURE 1: Solvent accessible pockets of the heterodimer and homodimer. The protein backbone is represented by the green (α subunit in the heterodimer and β^1 subunit in the homodimer) and blue (*β* subunit in the heterodimer and β^2 subunit in the homodimer) ribbons, and the surface (yellow inside, gray outside) is the cavity of the solvent accessible pocket. The arrow points to the opening of the pocket, and the *β*-His81 and α-Ala81 side chains are shown in red. (A) Heterodimer, where the outer portion of the solvent accessible pocket narrows between the *β*-His81 and α-Ala81 side chains before the channel widens again into the inner portion of the pocket. (B) Homodimer, where the two *β*-His81 side chains isolate the inner portion of the pocket from the solvent accessible outer portion.

Residue 89 in the inner portion of the solvent pocket is an aspartic acid in α and a glutamic acid in *β*. We constructed one double mutant heterodimer in which His81 of *β* was changed to alanine and Glu89 of *β* was changed to aspartic acid (*β*-H81A/E89D) to investigate the importance of the volume of the inner portion of the solvent accessible pocket (residue 89) along with the size of the outer portion of the pocket (residue 81). Figure 3A shows the opening of the solvent pocket in the heterodimer with the surface area contributed by the two residues at position 89 highlighted. Figure 3B shows the orientation of the side chains of these residues at position 89 relative to residues *β*-His81 and α-Ala81 and the solvent accessible pocket. This double mutant heterodimer is expected to have a larger solvent

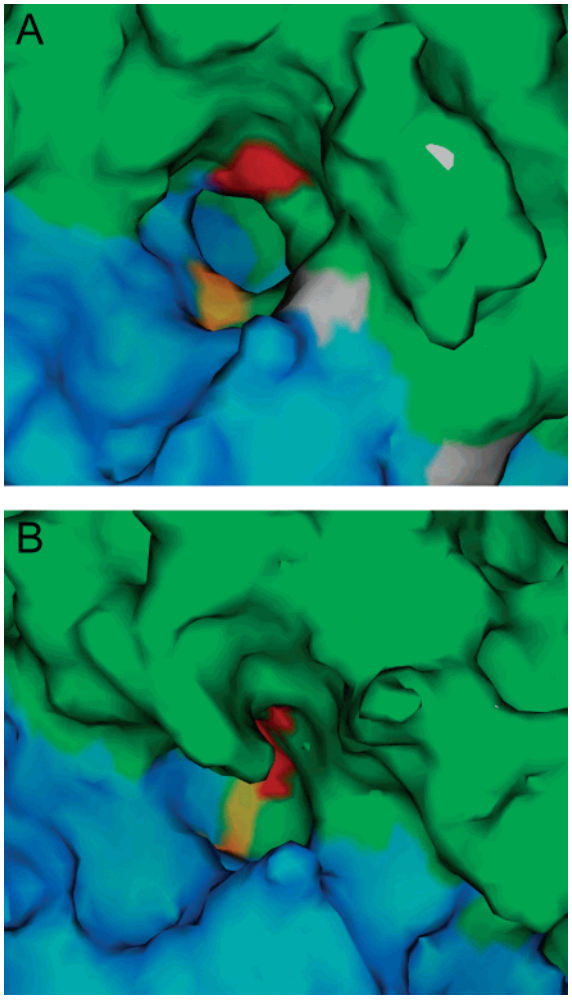

FIGURE 2: Surface structure of the solvent accessible pocket of the heterodimer and homodimer when looking straight into the pocket. (A) Heterodimer, where there is a narrow channel between β-His81 and α-Ala81 across the subunit interface and the inner portion of the pocket is visible behind these residues. The surface of α is shown in green and β in blue. The portions of the surface contributed by residues α-Ala81 and β-His81 are colored red and orange, respectively. (B) Homodimer, where the inner portion of the solvent pocket is not visible because the two β-His81 side chains form a barrier, isolating the outer portion of the cavity from the inner portion. The surface of one subunit is shown in green and the other in blue. The portions of the surface contributed by the two β-His81 residues are colored red and orange.

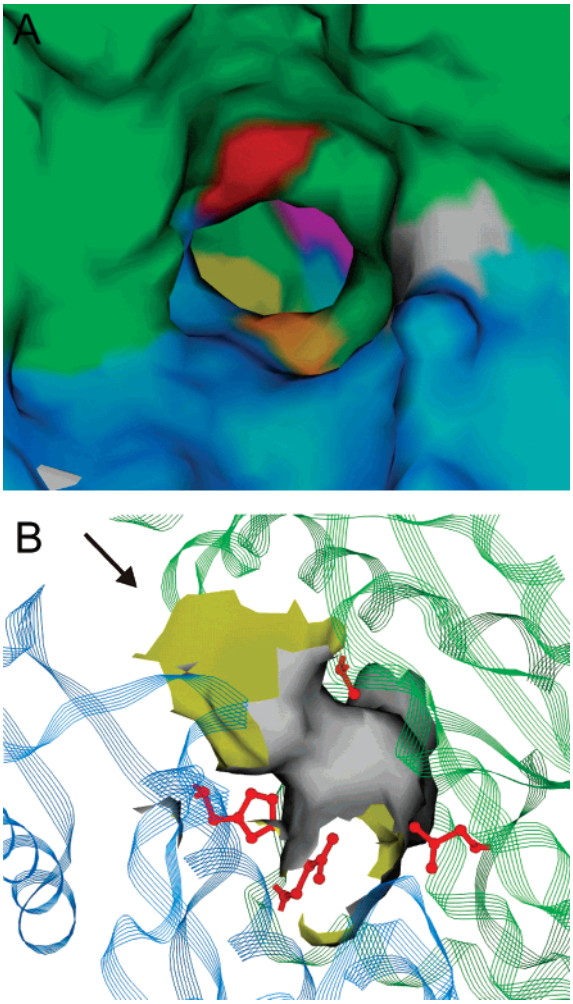

FIGURE 3: Relationship between residues 81 and 89 in the heterodimer. (A) Surface structure of the solvent accessible pocket, looking straight into the pocket. The surface of α is shown in green and β in blue. The surface areas contributed by α-Asp89 and β-Glu89, in purple and yellow, respectively, are partly visible in the inner portion of the pocket; the surface areas contributed by α-Ala81 and β-His81, in red and orange, respectively, form the narrow channel between the inner and outer portions of the pocket. (B) Orientation of the side chains of residues 81 and 89 around the solvent accessible pocket. The protein backbone is represented by the green (α subunit) and blue (β subunit) ribbons, and the surface (yellow inside, gray outside) is the cavity of the solvent accessible pocket. The arrow points to the opening of the pocket, and the β-His81, α-Ala81, β-Glu89, and α-Asp89 side chains are shown in red.

accessible pocket in both the outer portion (residue 81) and the inner portion (residue 89) than the wild-type heterodimer.

There is a hydrogen bond across the subunit interface between the backbone amide of β-Glu89 and the α-Asn54 side chain (*6*); mutation of the β-Glu89 side chain was not expected to disrupt this interaction. Residue 81 is not involved in hydrogen bonding in either subunit (*6*).

Residue 82 of both the α and β subunits is a conserved histidine in all species of luciferase with known sequences (*1*, *2*, *11*−*17*). In the *V. harveyi* luciferase heterodimer, there is an intersubunit hydrogen bond between the β-His82 side chain and the α-Val116 carbonyl (*6*). In the homodimer, only one of the His82 residues forms a hydrogen bond with the carbonyl of residue 116 of the other subunit (*7*). To investigate the importance of hydrogen bonding at the subunit interface and the role of this conserved histidine, we constructed the β-H82A mutant. This mutation prevents the formation of a hydrogen bond with α-Val116. Figure 4 shows the locations of β-His82 and α-Val116 in the heterodimer.

We will show here that each of the four subunit interface heterodimeric mutants unfolds by the same mechanism as the wild-type heterodimer. In addition, we found that none of the four subunit interface mutations has a measurable effect on the free energy difference associated with subunit dissociation during urea-induced unfolding extrapolated to water ($\Delta G_2^{H_2O}$). Three mutants (α-A81H, β-H81A, and β-H82A) exhibit lower $\Delta G_1^{H_2O}$ values for formation of the heterodimeric intermediate than the wild-type enzyme. Formation of the partially unfolded heterodimeric intermediate involves unfolding or partial loss of structure of the C-terminal domain (ca. residues 236−355) in 2 M urea (*18*, *19*).

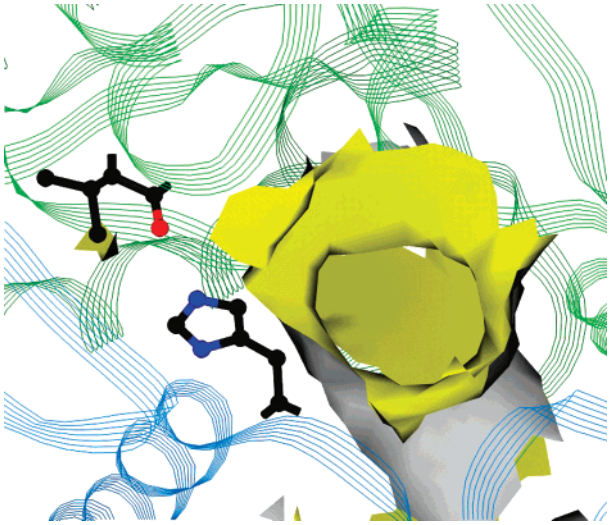

FIGURE 4: Side chain of β-His82, near the mouth of the solvent accessible pocket, forming a hydrogen bond across the subunit interface with the carbonyl of α-Val116. The protein backbone is represented by green (α subunit) and blue (β subunit) ribbons, and the solvent accessible pocket, viewed looking straight into the pocket, is the yellow and gray surface.

MATERIALS AND METHODS

Materials. Ultrapure urea was purchased from J. T. Baker and ICN Biomedicals, Inc., and NaH_2PO_4 and K_2HPO_4 were from EM Science. Bovine serum albumin and flavin mononucleotide (FMN) were obtained from Sigma; *n*-decyl aldehyde was from Aldrich, and EDTA and dithiothrietol (DTT) were from ICN Biomedicals, Inc. All other chemicals were reagent grade or higher.

Mutagenesis, Expression, and Protein Purification. The single-site mutations were made using the Stratagene QuikChange Site-Directed Mutagenesis Kit to mutate the *V. harveyi* wild-type Lux A or Lux B gene, which encodes α or β, respectively, in the pJHD500 plasmid. The double mutant, β-H81A/E89D, was made from the β-H81A mutant using the QuikChange kit procedure to add the E89D mutation.

Wild-type luciferase and each of the mutants were overexpressed in *Escherichia coli* and purified as described previously (*20*). The final concentration of protein stock solutions was determined by absorbance at 280 nm using an extinction coefficient of 1.136 mL mg^{-1} cm^{-1} for all mutants.

Enzyme Activity Measurements. Bioluminescence activity was measured using the $FMNH_2$ injection assay (*21*) and a luminometer (*22*). The assay was repeated 10−12 times for each mutant, and the results were averaged.

Analytical Ultracentrifugation. Sedimentation equilibrium experiments were carried out using a Beckman XL-A analytical ultracentrifuge. Samples were exhaustively dialyzed at 4 °C against 50 mM NaH_2PO_4/K_2HPO_4 buffer (pH 7.0) containing 100 mM NaCl and 0.5 mM DTT. Protein samples (A_{280} in the range of 0.2−0.6) with dialysate as a reference were allowed to come to equilibrium at 12 000 and 16 000 rpm at 18 °C. Scans of the absorbance at 280 nm as a function of radial position were taken using a 0.001 cm step size. Equilibrium was assumed to be reached when consecutive scans 4 h apart could be superimposed.

Sedimentation Equilibrium Data Analysis. Sedimentation equilibrium data were analyzed using a model for a single sedimenting species (eq 1)

$$C_r = C_0 \exp\{[M(1 - \nu\rho)\omega^2/2RT](r^2 - r_0^2)\} + E \quad (1)$$

where r is any radial position, C_r is the concentration determined from the A_{280} at radial position r, r_0 is the reference radial position, C_0 is the concentration at r_0, M and ν are the average molecular weight and partial specific volume, respectively, of the sedimenting species, ρ is the solvent density, ω is the angular velocity, R is the ideal gas constant, T is the absolute temperature, and E is the baseline offset. The partial specific volume, ν, of the heterodimer (0.729 mL/g) was calculated on the basis of amino acid composition (*1*). The value of ρ (1.008 g/mL) was determined from standard tables (*23*).

The Kaleidagraph program (Synergy Software, Reading, PA) was used to fit eq 1 to the equilibrium sedimentation data to obtain a molecular weight, M, for each of the mutants. The standard error of M for each mutant, sd_M, was calculated according to eq 2

$$sd_M = \sqrt{\sum_{i=1}^{n} \frac{sd_i^2}{n^2}} \quad (2)$$

where sd_i is the standard error of M obtained from the fit of eq 1 to a sedimentation data set at a particular protein concentration and angular velocity (condition i) and n is the number of data sets (each at a different protein concentration and/or angular velocity) analyzed. At least six different combinations of protein concentration and angular velocity were analyzed for each mutant.

Urea Equilibrium Denaturation Curves. Each urea equilibrium denaturation curve was generated from 30 unfolding and 13 refolding samples, all at either 10 or 25 μg/mL. Unfolding samples were prepared by mixing appropriate volumes of 50 mM NaH_2PO_4/K_2HPO_4 buffer (pH 7.0) containing 1 mM DDT with an appropriate volume of a 10 M urea stock in the same buffer, prepared according to Pace et al. (*24*), to make 2 mL samples which increased in urea concentration over the range of 0−7 M. After the buffer/urea mixtures were thoroughly vortexed and equilibrated at 18 °C in a water bath, 100 μL of either a 0.2 or 0.5 mg/mL protein stock at 18 °C was added while vortexing. Samples were returned to the 18 °C water bath and incubated overnight. Stocks of denatured protein at 0.2 and 0.5 mg/mL for the refolding samples were prepared in 7.0 M urea 1 day in advance and incubated overnight at 18 °C. Refolding samples were prepared, using the denatured protein stocks, by the same procedure and at the same time as the unfolding samples.

At least two sets of unfolding and refolding samples at each protein concentration (10 and 25 μg/mL) for each mutant were analyzed using an AVIV model SF202 spectropolarimeter by measuring the CD signal at 222 nm. A 0.5 cm quartz cell was used, and data points at 222 nm for each sample were collected every second for 15 s and averaged. The background signal at 222 nm was subtracted from each measurement.

At least two additional data sets at each protein concentration were analyzed using an SLM 8000 spectrofluorometer by measuring the tryptophan fluorescence at 324 nm. Fluorescence emission spectra were collected at 18 °C using a 1 cm quartz cell with excitation at 295 nm, monitoring emission from 306 to 400 nm. Background fluorescence was subtracted from all scans.

Data Analysis of Urea Denaturation Curves. Duplicate sets of data from experiments using the same protein concentration were combined for curve-fitting analysis; refolding data points were excluded from analysis due to scatter caused by aggregation in samples between 0 and 2 M urea. Equations describing the four-state unfolding model

$$(\alpha\beta)_N \overset{K_1}{\rightleftharpoons} (\alpha\beta)_I \overset{K_2}{\rightleftharpoons} \alpha_I + \beta_I \overset{K_3}{\rightleftharpoons} \alpha_U + \beta_U$$

were fit to the unfolding data. For simplicity, it was assumed that α_I and β_I each unfold to α_U and β_U, respectively, with the same equilibrium constant K_3. The IGOR Pro software (WaveMetrics, Inc.) which uses a nonlinear least-squares algorithm was used for preliminary curve fitting. The best estimates of the fitted parameters obtained with IGOR were then used as starting values of those parameters for final optimization and error analysis with the Stata 5.0 statistical software package (Stata Corp.). The equations describing the four-state model which were fit to the data were derived as follows.

The fractions of all species are given by eqs 3−6

$$f_N = \frac{N}{N_T} \tag{3}$$

$$f_I = \frac{I}{N_T} \tag{4}$$

$$f_X = f_{\alpha_I} = f_{\beta_I} = \frac{\alpha_I}{N_T} = \frac{\beta_I}{N_T} = \frac{X}{N_T} \tag{5}$$

$$f_S = f_{\alpha_U} = f_{\beta_U} = \frac{\alpha_U}{N_T} = \frac{\beta_U}{N_T} = \frac{S}{N_T} \tag{6}$$

where N_T represents the initial total protein concentration and $N = [(\alpha\beta)_N]$, $I = [(\alpha\beta)_I]$, $\alpha_I = [\alpha_I]$, $\beta_I = [\beta_I]$, $\alpha_U = [\alpha_U]$, and $\beta_U = [\beta_U]$. (Note that α_I and β_I are designated species X and α_U and β_U are designated species S.) The sum of the fractions of all species must equal 1 (eq 7).

$$f_N + f_I + f_X + f_S = 1 \tag{7}$$

The three equilibrium constants (K_1, K_2, and K_3) are defined in eqs 8−10, respectively.

$$K_1 = \frac{f_I}{f_N} \tag{8}$$

$$K_2 = \frac{f_X^2 N_T}{f_I} \tag{9}$$

$$K_3 = \frac{f_S^2}{f_X^2} \tag{10}$$

The spectroscopic signal of an unfolding or refolding sample at a given urea concentration, Y, is a linear combination of signals from the species present (eq 11)

$$Y = Y_N f_N + Y_I f_I + Y_X f_X + Y_S f_S \tag{11}$$

where Y_N, Y_I, Y_X, and Y_S are the intrinsic spectroscopic signals for species N, I, X, and S, respectively. To fit eq 11 to the equilibrium denaturation data over a range of urea concentrations, f_N, f_I, f_X, and f_S needed to be defined in terms of K_1, K_2, K_3, and N_T. By combining eqs 7 and 8, we found f_I (eq 12).

$$f_I = \frac{K_1 - K_1 f_S - K_1 f_X}{1 + K_1} \tag{12}$$

By combining eqs 9 and 12, we found f_X (13).

$$f_X = [-K_2K_1 + \sqrt{K_2^2K_1^2 - 4N_T(1 + K_1)(K_2K_1f_S - K_2K_1)}]/[2N_T(1 + K_1)] \tag{13}$$

By combining eqs 10 and 13, we found f_S (eq 14).

$$f_S = [-K_3^{-1/2}K_2K_1 - K_2K_1 + \sqrt{(K_3^{-1/2}K_2K_1 + K_2K_1)^2 + 4K_3^{-1}K_2K_1N_T(1 + K_1)}]/[2K_3^{-1}N_T(1 + K_1)] \tag{14}$$

K_1, K_2, and K_3 are all determined by their relation to the Gibbs free energy (eq 15)

$$K = \exp\left(\frac{-\Delta G}{RT}\right) \tag{15}$$

where R is the ideal gas constant and T is the absolute temperature. ΔG in eq 15 is assumed to be linearly dependent on urea concentration (eq 16)

$$\Delta G = \Delta G^{H_2O} - m[\text{urea}] \tag{16}$$

where ΔG^{H_2O} is the change in free energy for the equilibrium under consideration in the absense of denaturant. Y_I and Y_X in eq 11 were not further defined but were obtained directly from the fit of the expanded form of eq 11 to the data. Y_N and Y_S in eq 11 are defined by eqs 17 and 18 which describe the pre- and post-transition baselines, respectively, of the denaturation curve

$$Y_N = Y_{N'} + b_N[\text{urea}] \tag{17}$$

$$Y_S = Y_{S'} + b_S[\text{urea}] \tag{18}$$

where b_N and b_S are the slopes and $Y_{N'}$ and $Y_{S'}$ are the intercepts of these baselines. A linear dependence of the spectroscopic signal on urea concentration is assumed. The expanded form of eq 11, which incorporates eqs 8 and 12−18, was fit to the urea equilibrium denaturation data, and values of the thermodynamic parameters $\Delta G_1^{H_2O}$, $\Delta G_2^{H_2O}$, $\Delta G_3^{H_2O}$, m_1, m_2, and m_3 for the four-state model of unfolding were obtained.

Weighted average values for each thermodynamic parameter and its weighted standard error were calculated for each mutant using eq 19 by averaging the four values for each

Table 1: Enzymatic Activity of Bacterial Luciferase Variants[a]

luciferase	specific activity (quanta s^{-1} mg^{-1})	% of wild-type activity
wild type	3.2×10^{13}	
α-A81H	4.2×10^{12}	13
β-H81A	1.9×10^{13}	59
β-H82A	6.9×10^{12}	22
β-H81A/E89D	4.2×10^{12}	13

[a] Measured at 25 °C in 25 mM phosphate at pH 7.0 with ~0.05 mM *n*-decyl aldehyde as the substrate.

Table 2: Thermodynamic Parameters Obtained from Equilibrium Denaturation

protein	average thermodynamic parameter[a,b]	
wild type	$\Delta G_1^{H_2O} = 4.5 \pm 0.5$	$m_1 = 2.4 \pm 0.3$
	$\Delta G_2^{H_2O} = 20.3 \pm 1.9$	$m_2 = 4.3 \pm 0.7$
	$\Delta G_3^{H_2O} = 2.8 \pm 1.3$	$m_3 = 0.6 \pm 0.1$
α-A81H	$\Delta G_1^{H_2O} = 2.5 \pm 0.4$	$m_1 = 2.4 \pm 0.4$
	$\Delta G_2^{H_2O} = 20.0 \pm 3.0$	$m_2 = 4.2 \pm 0.6$
	$\Delta G_3^{H_2O} = 2.4 \pm 0.8$	$m_3 = 0.5 \pm 0.1$
β-H81A	$\Delta G_1^{H_2O} = 3.2 \pm 0.7$	$m_1 = 2.8 \pm 0.6$
	$\Delta G_2^{H_2O} = 19.4 \pm 5.6$	$m_2 = 3.8 \pm 1.0$
	$\Delta G_3^{H_2O} = 2.9 \pm 1.6$	$m_3 = 0.8 \pm 0.6$
β-H82A	$\Delta G_1^{H_2O} = 2.8 \pm 0.3$	$m_1 = 2.4 \pm 0.3$
	$\Delta G_2^{H_2O} = 19.2 \pm 2.6$	$m_2 = 4.0 \pm 0.4$
	$\Delta G_3^{H_2O} = 2.9 \pm 0.2$	$m_3 = 0.6 \pm 0.1$
β-H81A/E89D	$\Delta G_1^{H_2O} = 4.5 \pm 0.2$	$m_1 = 2.4 \pm 0.3$
	$\Delta G_2^{H_2O} = 19.6 \pm 13.5$	$m_2 = 3.9 \pm 1.3$
	$\Delta G_3^{H_2O} = 3.7 \pm 1.1$	$m_3 = 0.4 \pm 0.2$

[a] ΔG values in kilocalories per mole. [b] *m* values in kilocalories per mole per molar.

parameter obtained from curve fits to fluorescence data at 25 and 10 μg/mL and CD data at 25 and 10 μg/mL (Table 2). Weighting of the values was necessary because the standard error of each parameter varied depending on the protein concentration and the method used to collect the data (CD or fluorescence). In eq 19, w_i is the *i*th estimate calculated for parameter *w*, sd_{w_i} is the standard error of parameter w_i which was calculated by the fitting software, and *n* is the number of different observations ($n = 4$ in this case) of parameter *w*.

$$w = \frac{\sum_{i=1}^{n} \frac{w_i}{sd_{w_i}^2}}{\sum_{i=1}^{n} \frac{1}{sd_{w_i}^2}} \pm \sqrt{\frac{1}{\sum_{i=1}^{n} \frac{1}{sd_{w_i}^2}}} \qquad (19)$$

RESULTS

Activity of the Mutant Luciferases Relative to That of the Wild-Type Enzyme. The individual α and β subunits and the β_2 homodimer have essentially no activity (*3*, *4*, *25*, *26*). It is believed that the β subunit, when associated with α, stabilizes the active ensemble of conformers of α such that an efficient bioluminescence reaction is possible. Various lesions of both the α and β subunits of the enzyme have been characterized which have extremely low activity (reduction of several orders of magnitude). These mutations either cause changes to residues of the putative active site itself so that the bioluminescence reaction cannot occur [α-His44 and α-His45 mutants and AK α subunit mutants (*27*, *28*)] or to some extent compromise the structural stability necessary for activity which is imparted to α through association with a modified form of β [FB-1 β subunit mutant (*29*)]. The average specific activities for the wild type and the mutant luciferases investigated in this report are summarized in Table 1. All of these mutants show only modest reductions in activity relative to that of the wild type.

Mutations in the α subunit generally have a much more detrimental effect on activity than those in the β subunit (*27*); this is expected as the putative substrate binding site is located in the α subunit (*6*, *25*, *27*). Residue α-Ala81 is not sufficiently close to the putative active site to be involved directly in the bioluminescence reaction, but α-A81H did exhibit a modest reduction in activity to 13% of that of the wild type (Table 1).

Most single-site mutations which have been made in the β subunit result in no more than a 35% reduction in activity (*30*). The activities of β-H81A and β-H82A were reduced approximately this amount, to 59 and 22% of that of the wild type (Table 1), respectively. These numbers agree well with the previous report of 42 and 11% of wild-type activity for these mutants, respectively, considering the difference in the method for the assay (*30*). The double mutant of the β subunit, β-H81A/E89D, exhibited a greater reduction in activity than these two β mutants, to 13% of wild-type activity (Table 1), the same as α-A81H.

Dimer Molecular Weights from Analytical Ultracentrifugation. The model for a single sedimenting species of dimer molecular weight fit well to the data for the wild type and each of the mutants (residuals were random). The molecular weights obtained for the wild-type enzyme, α-A81H, β-H81A, β-H82A, and β-H81A/E89D were 75 433 ± 650, 76 859 ± 493, 76 735 ± 261, 76 364 ± 489, and 75 751 ± 440, respectively, agreeing well with the theoretical molecular weights of the dimers calculated from amino acid composition of 76 502, 76 568, 76 436, 76 436, and 76 422, respectively. These data suggested that the mutations did not alter the dissociation constant to an extent that can be measured, consistent with the fact that $\Delta G_2^{H_2O}$ for subunit dissociation did not change for any of the mutants relative to that of the wild type (see Table 2 and the Discussion).

Thermodynamic Parameters from Urea Denaturation Curves. Figure 5 shows the four-state model fit to wild-type and β-H82A denaturation data. The difference in the transition from 0 to 2 M urea where the dimeric intermediate is populated is apparent when comparing panels A and B of Figure 5. The average thermodynamic parameters obtained by fitting the four-state model to the urea denaturation curves for each of the mutants are listed in Table 2. The four-state parameters for the wild type were in good agreement with those reported previously from the three-state model (*9*). Given the standard errors of each of the parameters, only $\Delta G_1^{H_2O}$ values for formation of the dimeric intermediate for β-H81A, β-H82A, and α-A81H differ from that of the wild type. Interestingly, the decrease in $\Delta G_1^{H_2O}$ for mutants β-H82A and α-A81H is ~2 kcal/mol, close to the value of 2.3 kcal/mol of stabilization conferred to α by association with β (*18*). Consistent with the fact that there is no measurable change in K_D for subunit dissociation of the mutants relative to that of the wild type (only dimers observed by analytical ultracentrifugation), there is no statistically significant change in $\Delta G_2^{H_2O}$, the free energy

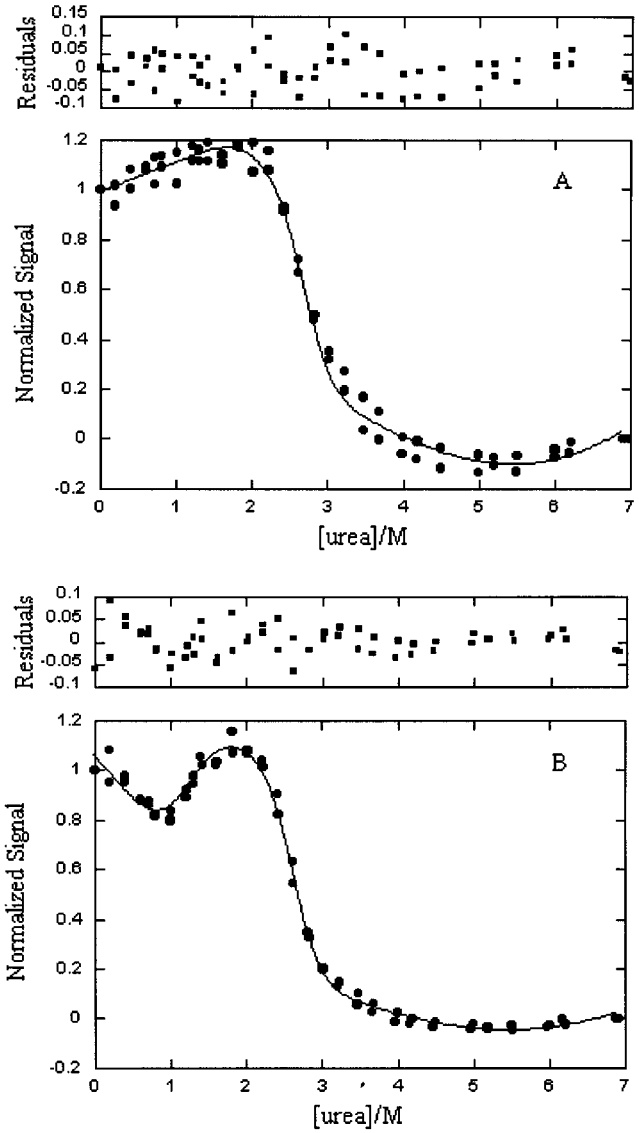

FIGURE 5: Four-state model fit to urea denaturation data determined by fluorescence emission at 25 μg/mL total protein. The solid line represents the nonlinear least-squares best fit of the model to the data using eq 11 as described in Materials and Methods: (A) wild type and (B) β-H82A.

change associated with subunit dissociation. This suggests that the mutations at the subunit interface did not alter the subunit−subunit interactions in a way that caused a measurable change in subunit binding affinity.

Because of the standard error of the data, we cannot conclude whether there is any difference in either Y_I or Y_X, the intrinsic spectroscopic signals for the dimeric intermediate and the largely unfolded subunits, respectively, for any of the mutants relative to that of the wild type (data not shown). We believe that the dissociated subunits retain only a small amount of structure, perhaps a hydrophobic cluster, so that we would expect Y_X to be the same for the wild type and all of the mutants. However, it is possible that Y_I differs between the proteins, although our data cannot confirm this suggestion.

DISCUSSION

Small Reduction in the Activity of Luciferase Mutants. The mutants characterized here exhibit only modest reductions in activity (Table 1) relative to the essentially inactive individual subunits (*3*, *4*, *26*). It is widely agreed that the active center of the enzyme resides on the α subunit (*6*, *25*, *27*). The role of the β subunit in the bioluminescence reaction is unknown, but we believe that it functions in some way to stabilize a conformation of α that is required for the bioluminescence reaction to occur. Mutation to the β subunit in the FB-1 mutant somehow precluded stabilization of the high quantum yield for α, decreasing the activity of this heterodimeric mutant to ~5% of the wild-type activity (*27*). It is interesting that the mutations characterized here do not cause greater loss in activity, as they all occur at the subunit interface where structural changes in β should be propagated to α. Apparently, these mutations do not disrupt to any significant extent the stabilizing forces imparted across the interface to α from β, and the bioluminescence reaction can occur, albeit with a somewhat lower efficiency.

Both β-His81 and β-His82 are conserved in all species of bacterial luciferase with known sequences (*1*, *2*, *11*−*17*). In addition, residues 64−106 (the region including residues 81 and 82) of the β subunit are the most similar across species in their predicted secondary structures (*30*). This may indicate that some structural feature of this region of the β subunit is necessary for the efficiency of the bioluminescence reaction occurring on the α subunit. The mutations in these two residues probably cause slight perturbations in the native structure of β which are propagated to α when the two subunits are associated, so that the ability of the α subunit to bind substrates or form the proper intermediates during the bioluminescence reaction is compromised, making the reaction slightly less efficient than in the wild-type heterodimer. The same is probably true of the α-A81H mutant. Residue 81 of α is not close enough to the putative active site to be involved in the bioluminescence reaction, but its mutation may cause structural perturbations which are propagated through the subunit to the active site, adversely affecting the efficiency of the reaction.

The mutation of β-Glu89 to aspartic acid along with the mutation of β-His81 to alanine has a more detrimental affect on activity than the histidine to alanine mutation alone (β-H81A, 59% of wild-type activity; β-H81A/E89D, 13% of wild-type activity; Table 1). The larger reduction in activity of β-H81A/E89D may be partly due to the proximity of β-Glu89 to β-Glu88. β-Glu88 forms a hydrogen bond across the subunit interface with α-His45; mutation of α-His45, which is located in a pocket adjacent to the hydrophobic pocket which is the proposed active site (*6*), greatly reduces enzyme activity (*28*). The mutation of β-Glu89 may cause local structural changes which compromise the ability of β-Glu88 to form a hydrogen bond with α-His45 and, thus, adversely affect the activity.

Mutants Exist as Dimers. The K_D of the wild-type luciferase heterodimer is too small to be measured, but has been calculated to be on the order of 10^{-19} M (*31*), an extremely tight association of the subunits. Due to the high affinity of the wild-type subunits for each other, there is essentially no dissociation of the dimer under nondenaturing conditions and the protein sediments in the analytical ultracentrifuge as a single dimeric species. Any changes in K_D resulting from the substitutions in the mutants were too small to be detected, as only dimers were observed by analytical ultracentrifugation.

A loop deletion mutant in which the mobile loop region of the α subunit was deleted displays an increase in K_D such that a monomer−dimer equilibrium is observed by analytical ultracentrifugation (*32*). This observation is of great interest with regard to the subunit interface mutants discussed here, because the deletion of the mobile loop, which does not contribute to the subunit interface, obviously has some effect on the interface interactions as shown by the increase in K_D values; in contrast, these mutations at the subunit interface show no measurable change in K_D from that of the wild-type heterodimer. It would appear from these observations that factors other than the volume of the solvent accessible channel at the subunit interface play a critical role in stabilizing the heterodimeric structure. Certainly, the extensive hydrophobic surface at the interface would be expected to confer significant stability, and these portions of the interface were not altered in these studies. However, the hydrophobic portions of the interface were not altered by deletion of the disordered loop either, but there was a large effect on the subunit equilibrium, demonstrating that subunit affinity is not due only to intersubunit interactions.

Luciferase Unfolding Can Be Described by a Four-State Model. Previous analyses of the unfolding and refolding of the bacterial luciferase heterodimer employed the three-state model (*9*).

$$(\alpha\beta)_N \overset{K_1}{\rightleftharpoons} (\alpha\beta)_I \overset{K_2}{\rightleftharpoons} \alpha_U + \beta_U$$

The urea denaturation experiments reported here were carried out to higher urea concentrations (7 M) than those of Clark et al. (*9*), and it became apparent that this model did not fit well at high urea concentrations. The four-state model which adds a third phase to the unfolding after dissociation of the subunits

$$(\alpha\beta)_N \overset{K_1}{\rightleftharpoons} (\alpha\beta)_I \overset{K_2}{\rightleftharpoons} \alpha_I + \beta_I \overset{K_3}{\rightleftharpoons} \alpha_U + \beta_U$$

described the data well. On the basis of an *F* test comparing the two models, the improvement in fit was statistically significant. Unfortunately, the four-state model had a shallow minimum resulting in large standard errors for the parameter estimates. Although we know the fourth state is needed to adequately model the data, the four-state model parameters cannot be estimated with high precision from our data.

The four-state model seems to be a reasonable mechanism because intermediates with residual structure at high concentrations of denaturant have been observed for other proteins, including human carbonic anhydrase and yeast phosphoglycerate kinase (*33*−*35*). The α subunit of tryptophan synthase, a single-domain $(\beta/\alpha)_8$ barrel, populates an intermediate at 5 M urea as evidenced by fluorescence anisotropy and one-dimensional (1D) proton NMR. It has been postulated that the structure of this intermediate consists of a hydrophobic cluster of some nonpolar side chains of the β-strands (*36*). In most proteins that retain residual structure at high concentrations of denaturant, the structure appears to involve sequences that are part of β-strands (*36*). This may also be the case for the monomeric α and β subunit intermediates of bacterial luciferase populated around 3.5 M urea.

Mutants Have m_3 and $\Delta G_3^{H_2O}$ Values That Are the Same as Those of the Wild-Type Heterodimer. The average values of m_3 and $\Delta G_3^{H_2O}$ for the mutants, reported in Table 2, show no difference from the corresponding values for the wild type, given the standard errors. The amount of buried surface area exposed upon unfolding has been shown to correlate with the *m* value of unfolding (*37*). According to the relationship determined by Myers et al., an *m* value of 0.6 kcal mol^{-1} M^{-1} (the average m_3 value for the wild type and the four mutants) corresponds to ∼2100 Å^2 of buried surface area becoming exposed. The change in buried surface area also correlates with the number of residues involved, so this change in exposed surface area involves approximately 32 residues. It is possible that there may be a core of ∼32 hydrophobic residues in the bacterial luciferase subunits which remain clustered together even under strongly denaturing conditions. Although it is in no way experimentally proven, we speculate that these residues could be the ones that come together first as the polypeptide chain folds, forming a stable core upon which the rest of the structure can be built.

It is not surprising that at high urea concentrations after dissociation and partial unfolding of the subunits has occurred there is no difference in the thermodynamics of unfolding for these mutants relative to the wild type. It is statistically unlikely that the one or two residues chosen for mutation (from the total of 679 residues in the two subunits) would be among the few which must be involved in the third transition of the four-state folding process.

Mutants Have m_2 and $\Delta G_2^{H_2O}$ Values That Are the Same as Those of the Wild-Type Heterodimer. The m_2 and $\Delta G_2^{H_2O}$ values for the mutants show no significant difference from the wild-type values. Since $\Delta G_2^{H_2O}$ and m_2 correspond to the dissociation and partial unfolding of the individual subunits, these data show that the mutations, although designed to affect the subunit interface, do not change the energetics related to dissociation of the two subunits. It may be possible to explain this lack of change in $\Delta G_2^{H_2O}$ by the fact that these mutations do not cause significant changes to the extensive hydrophobic surface of the subunit interface. The hydrophobic effect may contribute more to the affinity of the subunits for each other than the nature of the solvent accessible pocket at the interface, contrary to our original hypothesis. In the case of the β-H82A mutant, the loss of the intersubunit hydrogen bond to α-Val116 may be compensated by a new hydrophobic interaction with the alanine residue of the mutant β subunit, although it is unlikely that the loss of a single hydrogen bond would be observed, due to the error in the data.

β-H81A, β-H82A, and α-A81H Mutants Have Reduced $\Delta G_1^{H_2O}$ Values. The interesting difference between the mutants and the wild type is in the values of $\Delta G_1^{H_2O}$. The mutants β-H82A and α-A81H both show significantly reduced values (2.8 and 2.5 kcal/mol, respectively) relative to the value of 4.5 kcal/mol for the wild type. These single-site mutations lower the amount of energy needed for isomerization to the dimeric intermediate populated around 2 M urea so that the mutants are destabilized relative to the wild-type heterodimer. It has been shown that the α subunit alone has a $\Delta G_1^{H_2O}$ value of 2.24 ± 0.25 kcal/mol (*18*) which is essentially the same as the values for these mutants. It appears that the β-H81A protein has a slightly lower value

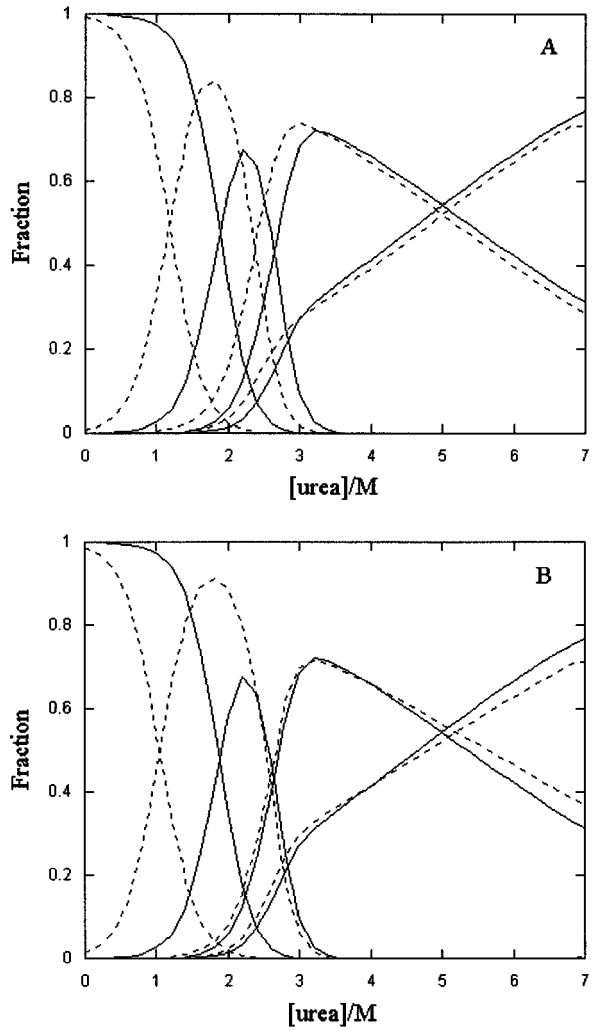

FIGURE 6: Theoretical population distribution of luciferase species at 25 μg/mL as a function of urea concentration. The fraction of each species was calculated using eqs 7 and 12−14 and the average thermodynamic parameters shown in Table 2. In both panels, the species present (in order of appearance with increasing urea concentration) are $(\alpha\beta)_N$, $(\alpha\beta)_I$, $(\alpha_I + \beta_I)$, and $(\alpha_u + \beta_u)$: (A) wild-type species (—) and β-H82A species (- - -) and (B) wild-type species (—) and α-A81H (- - -).

of $\Delta G_1^{H_2O}$ (3.2 ± 0.7 kcal/mol) than the wild type. Interestingly, β-H81A/E89D has a $\Delta G_1^{H_2O}$ value (4.5 ± 0.2 kcal/mol) nearly identical to that of the wild type. If indeed the $\Delta G_1^{H_2O}$ value for β-H81A were lower than that of the wild type, it would then appear that the effect of the mutation at position 81 is compensated by the mutation at position 89 in β-H81A/E89D. In general, mutation of two residues would be more likely to decrease the stability of the protein than only one mutation, but in this case, β-E89D could be a compensating mutation. The m_1 values for all the mutants were the same as that of the wild type (2.4 kcal mol^{-1} M^{-1}), given the standard errors, suggesting that the cooperativity and the amount of hydrophobic surface area exposed in the first unfolding phase of the four-state model are similar for all of these proteins.

Species distribution diagrams in Figure 6 from 0 to 7 M urea, generated using the average thermodynamic parameters in Table 2, display the effect of the reduced $\Delta G_1^{H_2O}$ values for β-H82A and α-A81H. The two mutants have an increased population of the intermediate, $(\alpha\beta)_I$, at lower urea concentrations than the wild type due to their lower $\Delta G_1^{H_2O}$ values.

Previous unfolding studies have shown that the C-terminal domain of the α subunit, which is the portion of the polypeptide chain away from the subunit interface, unfolds over the range of 0−2 M urea, leaving the dimeric intermediate, $(\alpha\beta)_I$, in which the N-terminal core of α remains folded (*18*, *19*). Since β-H81A, β-H82A, and α-A81H have reduced $\Delta G_1^{H_2O}$ values relative to that of the wild type, the mutations at the subunit interface must propagate through the structure of the α subunit, destabilizing the C-terminal portion of this subunit—the portion farthest from the subunit interface—so that less energy is required to reach the dimeric intermediate structure. It is interesting that the mutants β-H82A and α-A81H are destabilized so much that they display $\Delta G_1^{H_2O}$ values nearly the same as that of α alone (2.24 kcal/mol) (*18*). If a single mutation at the subunit interface in the N-terminal domain of the α subunit (α-A81H) or in the interface region of the β subunit (β-H82A and β-H81A) can cause a change in the thermodynamic parameter ($\Delta G_1^{H_2O}$) related to unfolding of the C-terminal domain at the other end of α, there must be very effective communication between the two domains of this subunit.

There is a clear difference between the native baselines that precede the transition from the native state to the dimeric intermediate state for the wild-type and mutant enzymes (Figure 5). As discussed above, formation of the dimeric intermediate involves unfolding of the C-terminal portion of the α subunit. Therefore, we must conclude that the effect of the mutations at the subunit interface, well removed from the C-terminal domain, must be transmitted through the structure of the α subunit. It is not surprising then that there is a difference in the perception of the chromophores being monitored by fluorescence and CD spectroscopies of the changing environment resulting from increasing the urea concentration in the solvent.

SUMMARY

All of the mutant heterodimers investigated here follow the same mechanism of unfolding as the wild-type luciferase heterodimer, namely, the four-state mechanism. The four mutations affecting the subunit interface of the heterodimer were conservative enough that the mechanism of unfolding did not change. In addition, the energetics of dissociation were not affected as $\Delta G_2^{H_2O}$ remained the same, and no mutants showed dissociation under native conditions by ultracentrifuge analysis. The α-A81H enzyme was designed so that its solvent accessible pocket is structurally more like that of the homodimer, with two histidine residues opposite each other across the interface. Since this mutant follows the same unfolding mechanism as the wild-type heterodimer, this feature of the subunit interface does not seem to contribute to the great difference in kinetic stability between the heterodimer and homodimer. Likewise, the changes to the size of the solvent accessible pocket for β-H81A and β-H81A/E89D and the loss of an intersubunit hydrogen bond in β-H82A did not change the mechanism of unfolding or the energetics of dissociation. We conclude, therefore, that the solvent accessible pocket at the subunit interface does not contribute in a major way to the stability of the

heterodimer and probably is not a major contributor to differences in the kinetic stability of the homodimer and heterodimer.

The three mutants β-H81A, β-H82A, and α-A81H reveal that the communication between the N- and C-terminal domains of the luciferase α subunit is very sensitive to small structural changes. The lower $\Delta G_1^{H_2O}$ values for these mutants demonstrate that mutations and their consequent structural changes can propagate across the subunit interface and through the α subunit to its C-terminal domain. This finding has implications for the activity of the wild-type heterodimeric enzyme. The role of the β subunit in the active enzyme is not known, but it seems to function by stabilizing a subset of conformations of α such that enzymatic activity is possible. These results lend further support to the idea that β communicates structural information across the subunit interface to the far regions of α, enabling the light-producing reaction to take place.

ACKNOWLEDGMENT

We thank Dr. Mark Inlow for statistical consultation, Dr. Joe Jilka for molecular biology advice, Drs. Brian Noland and Jonathan Sparks for help with the analytical ultracentrifugation experiments and helpful discussions, and Dr. J. Martin Scholtz for use of the CD spectrometer.

REFERENCES

1. Cohn, D. H., Mileham, A. J., Simon, M. I., Nealson, K. H., Rausch, S. K., Bonam, D., and Baldwin, T. O. (1985) *J. Biol. Chem. 260*, 6139−6146.
2. Johnston, T. C., Thompson, R. B., and Baldwin, T. O. (1986) *J. Biol. Chem. 261*, 4805−4811.
3. Waddle, J. J., and Baldwin, T. O. (1991) *Biochem. Biophys. Res. Commun. 178*, 1188−1193.
4. Sinclair, J. F., Waddle, J. J., Waddill, E. F., and Baldwin, T. O. (1993) *Biochemistry 32*, 5036−5044.
5. Sinclair, J. F., Ziegler, M. M., and Baldwin, T. O. (1994) *Nat. Struct. Biol. 1*, 320−326.
6. Fisher, A. J., Thompson, T. B., Thoden, J. B., Baldwin, T. O., and Rayment, I. (1996) *J. Biol. Chem. 271*, 21956−21968.
7. Thoden, J. B., Holden, H. M., Fisher, A. J., Sinclair, J. F., Wesenberg, G., Baldwin, T. O., and Rayment, I. (1997) *Protein Sci. 6*, 13−23.
8. Baldwin, T. O., Ziegler, M. M., and Powers, D. A. (1979) *Proc. Natl. Acad. Sci. U.S.A. 76*, 4887−4889.
9. Clark, A. C., Sinclair, J. F., and Baldwin, T. O. (1993) *J. Biol. Chem. 268*, 10773−10779.
10. Clark, C. A., Raso, S. W., Sinclair, J. F., Ziegler, M. M., Chaffotte, A. F., and Baldwin, T. O. (1997) *Biochemistry 36*, 1891−1899.
11. Baldwin, T. O., Chen, L. H., Chlumsky, L. J., Devine, J. H., Johnston, T. C., Lin, J.-W., Sugihara, J., Waddle, J. J., and Ziegler, M. M. (1987) in *Flavins and Flavoproteins* (Edmondson, D. E., and McCormick, D. B., Eds.) pp 621−631, Walter de Gruyter & Co., Berlin.
12. Foran, D. R., and Brown, W. M. (1988) *Nucleic Acids Res. 16*, 777.
13. Illarionov, B. A., Protopopova, M. V., Karginov, V. A., Mertvetsov, N. P., and Gitelson, J. I. (1988) *Nucleic Acids Res. 16*, 9855.
14. Szittner, R., and Meighen, E. (1990) *J. Biol. Chem. 265*, 16581−16587.
15. Johnston, T. C., Rucker, E. B., Cochrum, L., Hruska, K. S., and Vandegrift, V. (1990) *Biochem. Biophys. Res. Commun. 170*, 407−415.
16. Meighen, E. A. (1991) *Microbiol. Rev. 55*, 123−142.
17. Xi, L., Cho, K.-W., and Tu, S.-C. (1991) *J. Bacteriol. 173*, 1399−1405.
18. Noland, B. W., Dangott, L. J., and Baldwin, T. O. (1999) *Biochemistry 38*, 16136−16145.
19. Apuy, J. L., Park, Z.-Y., Swartz, P. D., Dangott, L. J., Russell, D. H., and Baldwin, T. O. (2001) *Biochemistry 40*, 15153−15163.
20. Baldwin, T. O., Chen, L. H., Chlumsky, L. J., Devine, J. H., and Ziegler, M. M. (1989) *J. Biolumin. Chemilumin. 4*, 40−48.
21. Hastings, J. W., Baldwin, T. O., and Nicoli, M. Z. (1978) *Methods Enzymol. 57*, 135−152.
22. Mitchell, G. W., and Hastings, J. W. (1971) *Anal. Biochem. 39*, 243−250.
23. Laue, T. P., Bhairavi, D. S., Ridgeway, T. M., and Pelletier, S. L. (1992) in *Analytical Ultracentrifugation in Biochemistry and Polymer Science* (Harding, S. E., Rowe, A. J. H., and Horton, J. C., Eds.) pp 63−89, The Royal Society of Chemistry, Cambridge, U.K.
24. Pace, C. N., Shirley, B. A., and Thomson, J. A. (1989) in *Protein Structure, A Practical Approach* (Creighton, T. E., Ed.) pp 311−330, IRL Press, New York.
25. Balwin, T. O., and Ziegler, M. M. (1992) in *Chemistry and Biochemistry of Flavoenzymes* (Muller, F., Ed.) Vol. III, pp 467−530, CRC Critical Reviews in Biochemistry, CRC Press, Boca Raton, FL.
26. Choi, H., Tang, C.-K., and Tu, S.-C. (1995) *J. Biol. Chem. 270*, 16813−16819.
27. Cline, T. W., and Hastings, J. W. (1972) *Biochemistry 11*, 3359−3370.
28. Xin, X., Xi, L., and Tu, S.-C. (1991) *Biochemistry 30*, 11255−11262.
29. Anderson, C., Tu, S.-C., and Hastings, J. W. (1980) *Biochem. Biophys. Res. Commun. 95*, 1180−1186.
30. Xin, X., Xi, L., and Tu, S.-C. (1994) *Biochemistry 33*, 12194−12201.
31. Baldwin, T. O., Ziegler, M. M., Sinclair, J. F., Clark, A. C., and Chaffotte, A.-F. (1993) in *Flavins and Flavoproteins* (Yagi, K., Ed.) pp 823, Walter de Gruyter & Co., Berlin.
32. Sparks, J. M., and Baldwin, T. O. (2001) *Biochemistry 40*, 15436−15443.
33. Martensson, L. G., Jonsson, B. H., Freskgard, P. O., Kihlgren, A., Svensson, M., and Carlsson, U. (1993) *Biochemistry 32*, 224−231.
34. Svensson, M., Johansson, P., Freskgard, P. O., Jonsson, B. H., Lindgren, M., Martensson, L. G., Gentile, M., Boren, K., and Carlsson, U. (1995) *Biochemistry 34*, 8606−8620.
35. Garcia, P., Merola, F., Receveur, V., Blandin, P., Minard, P., and Desmadril, M. (1998) *Biochemistry 37*, 7444−7455.
36. Gualfetti, P. J., Osman, B., and Matthews, C. R. (1999) *Protein Sci. 8*, 1623−1635.
37. Myers, J. K., Pace, C. N., and Scholtz, J. M. (1995) *Protein Sci. 4*, 2138−2148.

BI012113G